Advances in Surface-Enhanced Fluorescence

Joseph R. Lakowicz,[1,2] **Chris D. Geddes,**[1,2] **Ignacy Gryczynski,**[1] **Joanna Malicka,**[1] **Zygmunt Gryczynski,**[1] **Kadir Aslan,**[1] **Joanna Lukomska,**[1] **Evgenia Matveeva,**[1] **Jian Zhang,**[1] **Ramachandram Badugu,**[1] **and Jun Huang**[1]

We report recent achievements in metal-enhanced fluorescence from our laboratory. Several fluorophore systems have been studied on metal particle-coated surfaces and in colloid suspensions. In particular, we describe a distance dependent enhancement on silver island films (SIFs), release of self-quenching of fluorescence near silver particles, and the applications of fluorescence enhancement near metalized surfaces to bioassays. We discuss a number of methods for various shaped silver particle deposition on surfaces.

KEY WORDS: Silver island films; colloids; fluorescence; nanotechnology; radiative decay engineering; metal-enhanced fluorescence; photonic mode density.

INTRODUCTION

The first experimental and theoretical reports on metal-enhanced fluorescence in the 70's and 80's [1–6] have been overshadowed by the large signal enhancements seen with surface-enhanced Raman scattering (SERS) [7–12]. This approach offers signal enhancements of a factor of 10^3–10^5, and still more on specific "hot spots," allowing the detection of a single molecule [13] and even a single DNA base from the SERS signals [14]. Efficient SERS requires close contact of the studied molecules with the metallic surface, a distance below 20–30 Å. At this distance, the eventual fluorescence of molecules is significantly quenched, primarily by energy transfer to the metal surface. Much smaller enhancements of the fluorescence have been observed than those in SERS. We recently realized that high fluorescence enhancements should be possible for fluorophores deposited near metal particles under carefully optimized conditions [15–18]. Our first attempts were done with bulk solutions of fluorophores placed between two metalized slides. Although dominant parts of

fluorophores were left unaffected, we observed enhancements of a several fold [19–21]. This inspired us to proceed with systems where fluorophores were located at better defined distances to silver particles. These systems included labeled proteins [22] and DNA oligomers deposited on 3-aminopropyltriethoxysilane (APS) or polylysine [23,24] as monolayers. The structures of the used cyanine-dye labeled DNA, the absorption spectrum of SIFs, and the experimental arrangements are shown in Fig. 1. The emission spectra of Cy-dyes on APS-treated slides with and without SIFs are shown in Fig. 2. The recorded enhancements are about 5 and 7-fold for Cy3-DNA and Cy5-DNA,

ABBREVIATIONS: AFM, atomic force spectroscopy; APS, 3-aminopropyltriethoxysilane; BSA, bovine serum albumin; Cy3, N,N'-(dipropyl)-tetramethylindocarbocyanine; Cy5, N,N'-(dipropyl)-tetramethylindodicarbocyanine; DNA, deoxyribonucleic acid; dsDNA, double stranded deoxyribonucleic acid; Fl-DNA, fluorescein-deoxyribonucleic acid; DNA-SH, thiolated deoxyribonucleic acid; Fl-IgG, fluorescein-immunoglobulin G; Fl-HSA, fluorescein-human serum albumin; HSA, human serum albumin; ICG, Indocyanine Green; ITO, indium tin oxide; L, molar ratio of fluorophore to protein molecule; MEF, metal-enhanced fluorescence; OD, optical density; PCR, polymerase chain reaction; Q, quartz; RET, resonance energy transfer; SCCS, silver colloid coated surfaces; SEF, surface-enhanced fluorescence; SERS, surface-enhanced Raman scattering; SIFs, silver island films; ssDNA, single stranded deoxyribonucleic acid; TR-BSA, Texas Red-bovine serum albumin.
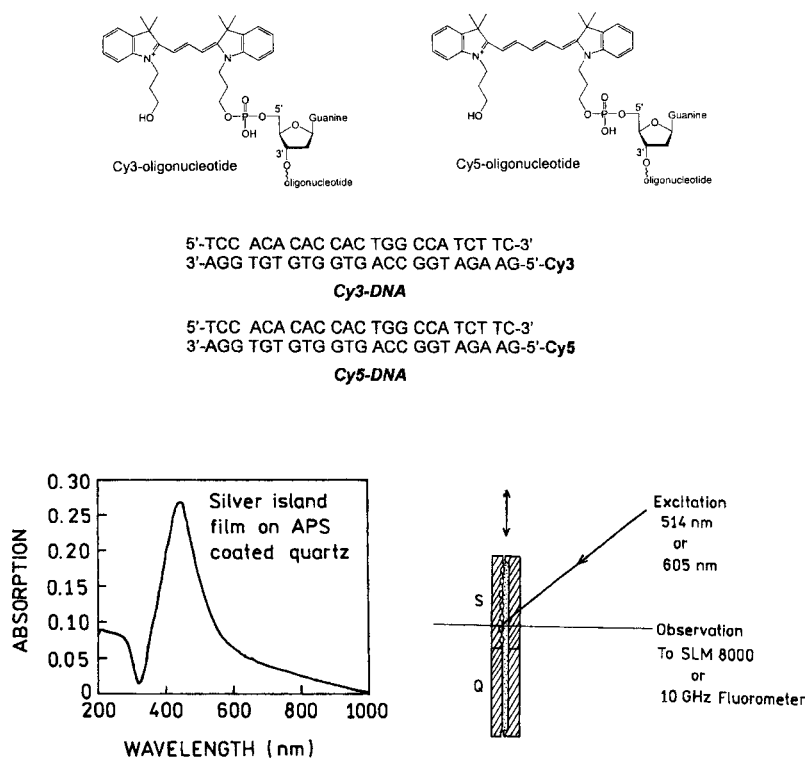
Fig. 1. DNA structures and sample geometry. Structures and sequences of the labeled and unlabeled DNA oligomers (top). Absorption spectrum of silver islands on APS and experimental geometry (bottom).

respectively. We also measured lifetimes of the deposited Cy-DNA monolayers and found that lifetimes on silvered slides are much shorter than on their unsilvered counterparts (Fig. 3). The simultaneous increase of quantum

Fig. 2. Emission spectra of Cy3-DNA (top) and Cy5-DNA (bottom) with and without silver island films.

efficiency and decrease of lifetime indicates an increased radiative decay rate in the presence of silver particles. In order to describe the interaction between fluorophore and metal particle, several factors should be taken into account.

In close proximity, up to ~ 50 Å, fluorophore emission is strongly quenched by metallic surfaces. The emission of fluorophores near the SIF but outside the quenching region is dependent on two major factors: an enhanced local field and an increase of the intrinsic decay rate of the fluorophore. The first factor provides stronger excitation rates. The second factor changes the quantum yield and lifetime of the fluorophore. The observed fluorescence enhancement

$$G \sim G_{ex} G_{QY}, \qquad (1)$$

where $G_{QY} = Q_m/Q_0$ is the increase in quantum yield of the fluorophore near a SIF.

Scheme 1 shows the energy diagrams for molecules in the absence and presence of SIFs. In the absence of SIFs, the quantum yield and lifetime are given by

$$Q_0 = \Gamma/(\Gamma + k_{nr}), \qquad (2)$$
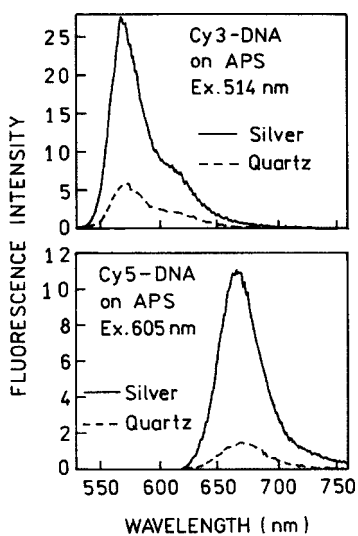
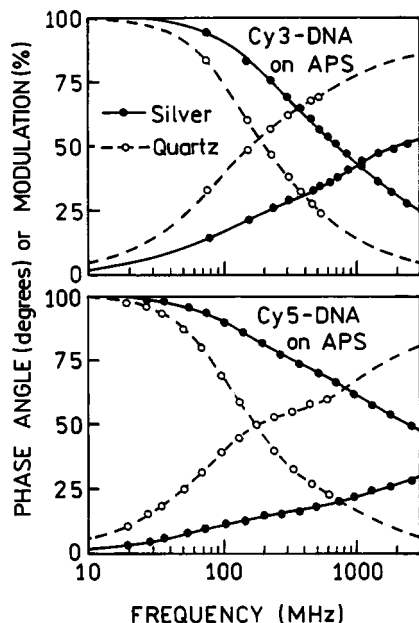$$\tau_0 = 1/(\Gamma + k_{nr}), \qquad (3)$$

Fig. 3. Frequency-domain intensity decays of Cy3-DNA and Cy5-DNA with (●) and without (○) SIFs.

where Γ is the radiative rate and k_{nr} are the nonradiative decay rates. In the presence of SIFs, the quantum yield and lifetime are given by

$$Q_m = \frac{\Gamma_m}{\Gamma_m + k'_{nr}}, \qquad (4)$$

$$\tau_m = \frac{1}{\Gamma_m + k'_{nr}}, \qquad (5)$$

where Γ_m and k'_{nr} are radiative and nonradiative rates in presence of metal particles. Increases in radiative rates ($\Gamma_m > \Gamma$) near SIFs result in increased quantum yields and decreased lifetimes. For more details on surface-enhanced fluorescence see [15]. The modifications of k_{nr} by metal are assumed negligible.

It is of interest to consider the increased signal that could be obtained using silver-coated surfaces. The total
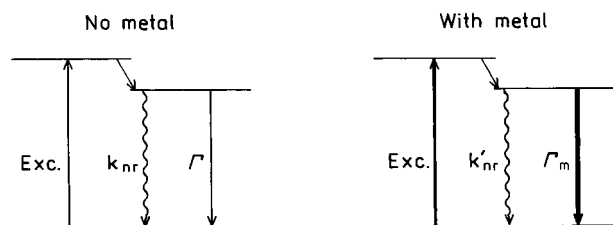
Schme 1. Jablonski diagram for molecules in absence (left) and presence (right) of metal particles.

detectable emission from a fluorophore is usually limited by its photostability [25,26]. Photochemical degradation occurs in the excited state so that a decreased lifetime should allow the fluorophore to undergo more excitation-deexcitation cycles before photobleaching. Therefore, we examined the emission intensity of Cy3-DNA tethered to APS slides and Cy5-DNA with continuous illumination (Fig. 4). These traces of intensity versus time were obtained with the same incident intensity so that the time-zero values represent the increased intensities shown in Fig. 2. If the time-zero values are normalized then the relative rates at which the emission decreases are about the same on quartz or silver regions of the slides. This result means that the increased intensity found on the silvered slide is not obtained at the expense of more rapid photobleaching. The relative areas under these curves (I_m/I_0) are 4.8 and 6.5 for Cy3 and Cy5, respectively. In other words, in this experiment it was possible within 5 min to extract 4.8 and 6.5 times more photons from silvered areas for Cy3-DNA and Cy5-DNA, respectively. Thus, the use of substrates coated with silver particles can result in a substantial increase in the signal observed from cyanine-labeled DNA. In Fig. 4, we present photobleaching data with the excitation power adjusted to yield the same emissive photon flux at time-zero. These data also show that the number of extracted photons within the time of measurement is higher on the silvered areas than on quartz alone.

In this experiment, there was limited control of the distance between the metal and the fluorophores, and fluorophores were probably present in areas outside the regions where enhanced emission was obtained. In the experiments described below, we will focus on increased brightness, lifetime shortening, and improved photostability.

NEW RESULTS FOR SURFACE-ENHANCED FLUORESCENCE

Distance-Dependent Enhancement

The interaction of fluorophores with metallic particles has been the subject of several publications [27–29]. There is reasonable agreement that the maximal enhancements occur about 100 Å from the surface, but some publications report the optimal distance to be as large as 600 Å [30]. In our opinion the use of metallic particles to enhance fluorescence has great potential for advances in medical diagnostics and biotechnological methodology [15]. For this reason, we examined the effects of metal-to-fluorophore distance on enhancement of fluorescence.
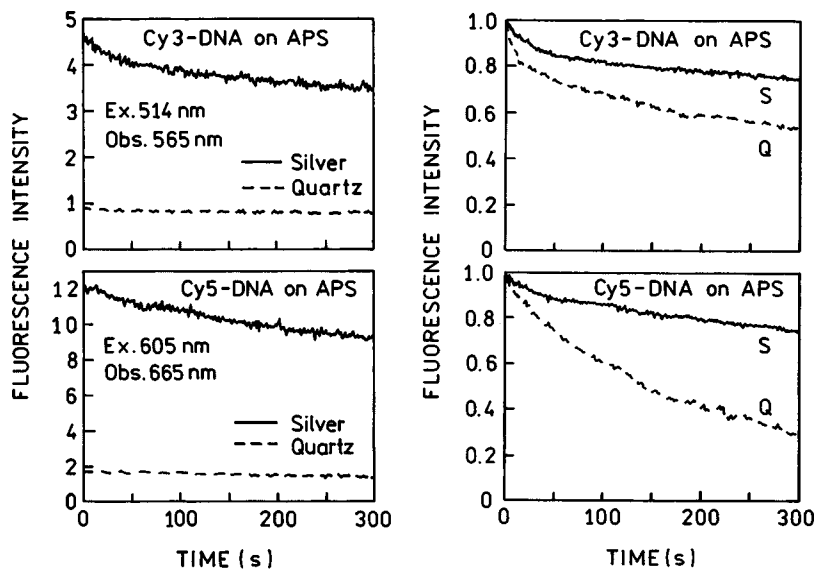
Fig. 4. Photostability of Cy3-DNA and Cy5-DNA on APS-treated slides, with and without silver island films, for the same incident power (left), and the excitation intensity adjusted to yield the same emission intensities on quartz and silver (right). Figures 1–4 are adopted from [24].

To investigate this distance dependence, we used alternating monolayers of biotinylated bovine serum albumin (BSA) and avidin (Scheme 2). It is known that BSA adsorbs as a monolayer onto glass or silver surfaces, and that subsequent exposure to avidin and then biotinylated BSA results in additional monolayers of these proteins [30]. Because of the relevance of genomic analysis, we examined dsDNA oligomers labeled with Cy3 or Cy5 (Fig. 1). An unlabeled biotinylated oligomer was used to bind the outermost layer of avidin. This biotinylated oligomer was previously hybridized to a complementary

oligomer labeled with Cy3 or Cy5. For a more detailed description of the multilayer preparation, we refer the readers to [31].

The SIFs used in this experiment display characteristic absorption (Fig. 5, top) which indicates most of the particles are subwavelength in size. Atomic force microscopy (AFM) revealed that most of the silver particles were about 500 nm wide and less than 100 nm high (Fig. 5, bottom). We used absorption spectra to determine the amounts of BSA and avidin bound to the uncoated slides and on the SIFs. Using the density of avidin expected for monolayer
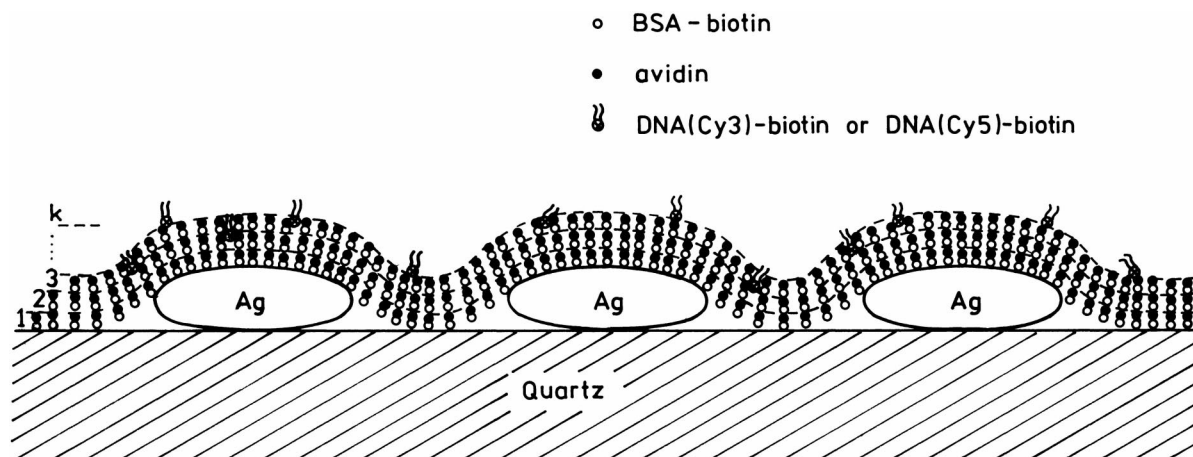
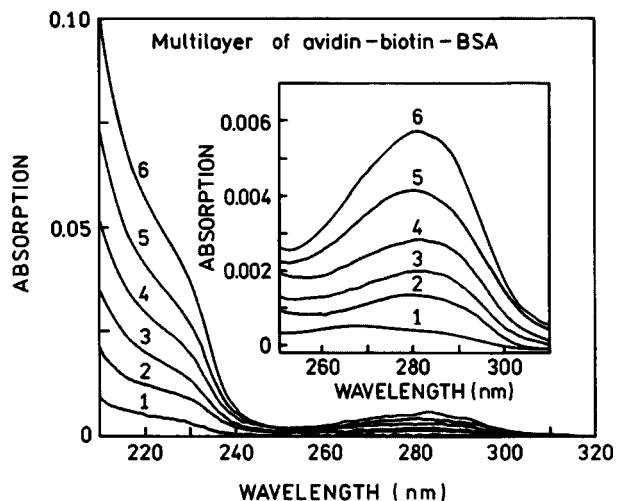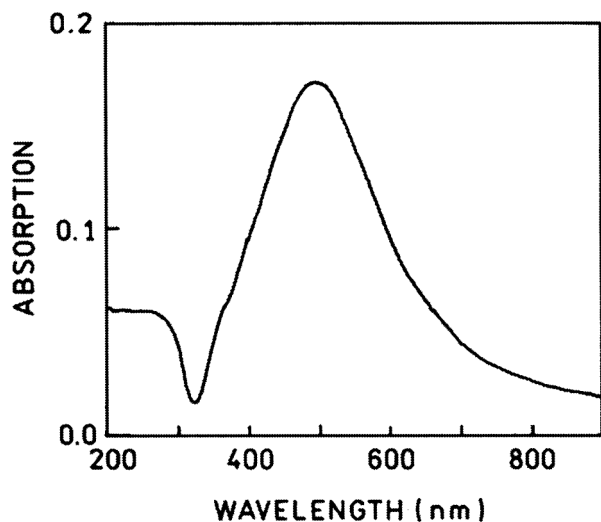**Scheme 2.** Schematic of BSA-avidin monolayers with labeled DNA.

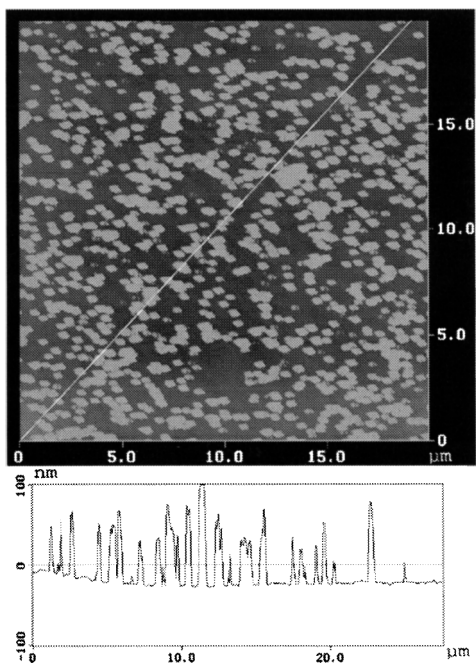**Fig. 6.** Absorption spectra of BSA-biotin-avidin layers.

Fig. 5. Absorption spectrum (top) and AFM image (bottom) of a representative SIFs.

Fig. 7. Emission spectra of DNA(Cy3)-biotin (top) and DNA(Cy5)-biotin (bottom) on BSA-biotin-avidin layers. Spectra are normalized to the spectrum on quartz (Q) with the same numbers of protein layers.

coverage [32], we calculated an optical density of 0.001 for each layer of BSA-biotin-avidin. Absorption spectra are shown in Fig. 6 for 1 to 6 BSA-biotin-avidin layers on quartz. The optical density increases linearly with the number of protein layers, and the OD is consistent with an almost complete monolyer of each protein.

To determine the effects of SIFs on fluorescence we exposed the protein-coated slides to DNA(Cy3)-biotin or DNA(Cy5)-biotin. Emission spectra are shown in Fig. 7 for the Cy3- and Cy5-labeled oligomers. The highest in-
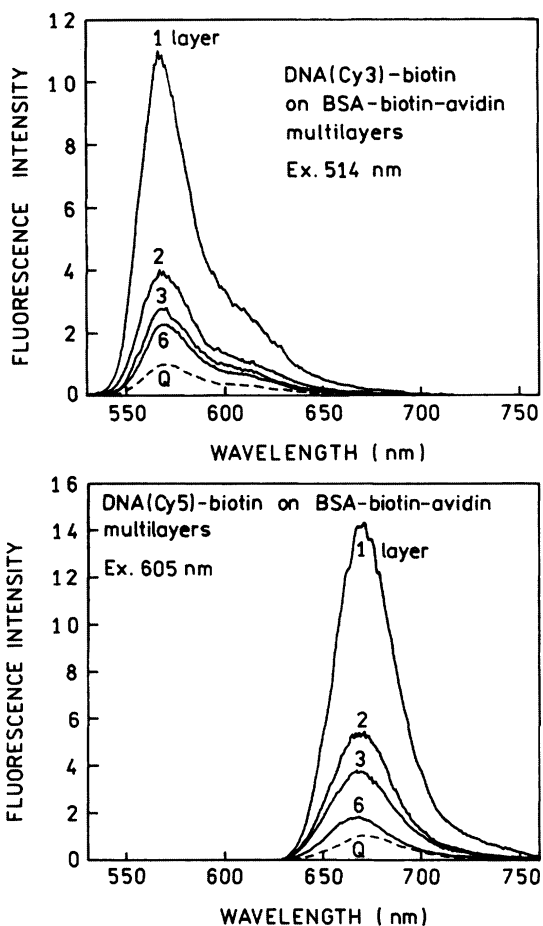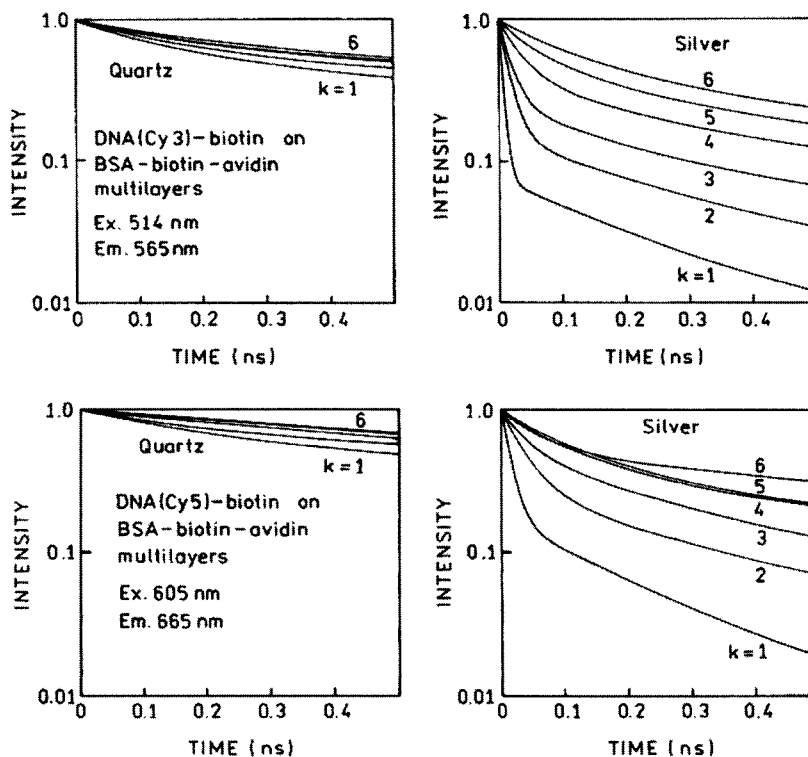
Fig. 8. Time-domain representation of emission intensity decays of DNA(Cy3)-biotin (top) and DNA(Cy5)-biotin (bottom) on BSA-biotin-avidin multilayers deposited on quartz (left) and SIFs (right).

tensity is seen for the labeled DNA bound to a single layer of BSA-biotin-avidin. The intensity, relative to uncoated quartz, decreases progressively with the number of protein layers to an enhancement near 2 for six layers. We note that the intensities were measured relative to that found for the labeled oligomers on quartz with the same number of protein layers.

We measured the frequency-domain intensity decays of Cy3- and Cy5-labeled oligomers with increasing numbers (k) of protein layers (Fig. 8). For both probes the frequency responses were most shifted to higher frequencies for the first protein layers, with the smallest shift found for six layers. In both cases the silver island films result in a short decay time component in the intensity decays, the amplitude of which is largest for the smaller number of protein layers. In contrast, the intensity decays on quartz are mostly independent of the number of protein layers. The intensity enhancements and ratios of amplitude-weighted lifetimes for Cy3 and Cy5 with different numbers of protein layers are shown in Fig. 9. The largest enhancements and shortest lifetimes were found for the first layer of BSA-biotin-avidin. The effect decreases more than 50% for the second layer and is essentially constant for the next four protein layers. We believe that

the effect is minimal in the third and higher layers, and the residual effects above four layers are due to labeled oligomers which penetrate into the protein underlayers. The distance-dependent enhancement data can be fitted
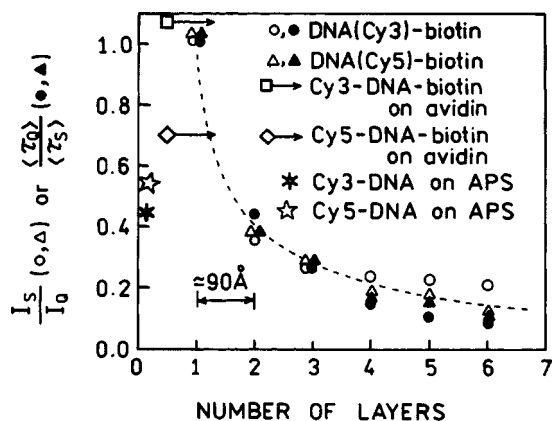

Fig. 9. Fluorescence enhancements of Cy3- and Cy5-labeled oligomers for various distances from the silver surface. Also shown are the enhancements found on amine-coated slides which were treated with APS and slides with a single layer of avidin. Figures 5–9 are adopted from [31].

with a phenomenological model which accounts for expected interactions [31].

Release of Self-Quenching

Self-quenching of fluorescein and other xantene-type dyes is one of the oldest observations in fluorescence and is due to resonance energy transfer between fluorescein molecules (homoRET). This process was frequently studied by decreases in the quantum yield and polarization or anisotropy of viscous solutions with high probe concentrations [33–38]. In the case of fluorescein, the Forster distance for homoRET is about 42 Å [39]. Since this distance is comparable to or larger than the size of many proteins, RET is expected to occur only when a macromolecule contains more than a single fluorophore. This phenomenon is particularly important for labeled antibodies used in immunoassays, where self-quenching of fluorescein limits the brightness available per labeled protein [40]. In some cases the phenomenon of self-quenching is turned into an advantage and has been used to study protein folding [41], distance measurements [42], or macromolecule association reactions [43–44].

One widespread use of fluorescein is in fluorescence immunoassays, which are widely used in clinical diagnostics and research [45–48]. In this application it is desirable that the labeled antibodies be as bright as possible for maximal sensitivity and observability over sample autofluorescence. However, the obvious approach to increasing the molecule brightness by increasing the extent of labeling is not useful due to self-quenching. We observed that self-quenching can be partially released in systems deposited on silvered surfaces [49–51]. Figure 10 shows the experimental setup for the study of fluorescence enhancements in fluorescein-labeled immunoglobulin G (Fl-IgG). Similar setups have been used in studies of fluorescein-labeled human serum albumin (HSA) [49] and DNA [50]. The emission spectra of Fl-IgG at different degrees of labeling are presented in Fig. 11, where L is molar ratio of fluorophore to protein molecule. The strongest increase in brightness (about 40) was observed for the highest labeling ($L = 25.6$). The dependence of enhancement on labeling is shown in Fig. 12. Up to about 10 fluoresceins per IgG molecule ($L = 10$), there is little dependence of enhancement on labeling, whereas HSA and 23 mer DNA already display a release of self-quenching at about $L = 3$. The IgG molecule is much larger than HSA, and the average distance between fluoresceins is greater in IgG than in HSA for the same degree of labeling. The lifetimes measured for low and high labeling of Fl-IgG are shown in Fig. 13. The lifetimes on SIFs are significantly decreased. However,
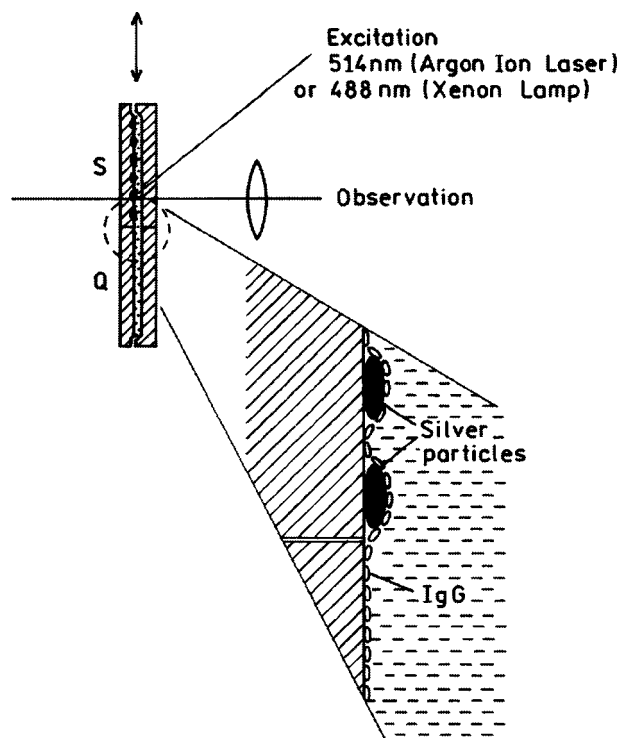

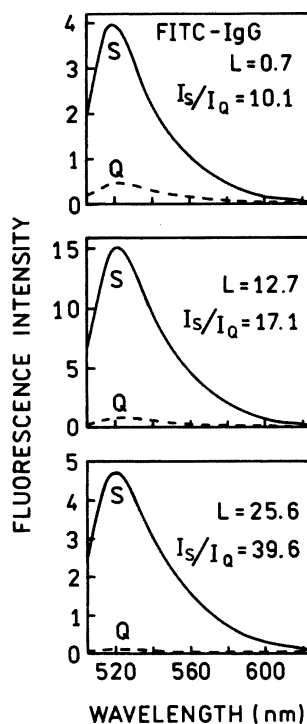**Fig. 10.** Experimental setup used in release of self-quenching study.

Fig. 11. Emission spectra of Fl-IgG on quartz (- - -) and silver (—) for $L = 0.7$, 12.7 and 25.6. Excitation was 488 nm.
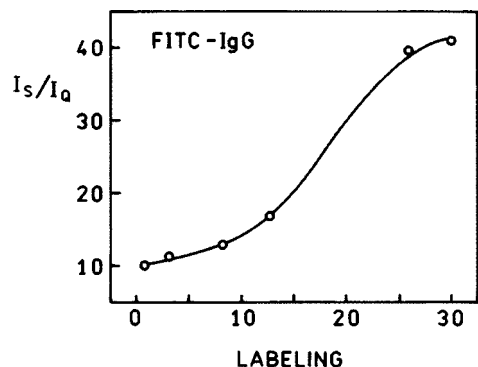
Fig. 12. The dependence of brightness enhancement on labeling.

a stronger change in lifetime was observed for low labeling ($\langle\tau\rangle_{\mathrm{SIF}}/\langle\tau\rangle_Q = 25$) than for high labeling ($\langle\tau\rangle_{\mathrm{SIF}}/\langle\tau\rangle_Q = 19$). This confirms that there is less self-quenching on SIFs.

DNA Hybridization Assays

Detection of DNA hybridization is the basis of a wide range of biotechnology and diagnostic applications [52]. DNA hybridization is measured on gene chips [53,54], during PCR [55,56], and for fluorescence *in situ* hybridization [57], to name a few. In all these applications increased sensitivity is desirable, particularly for detection of a small number of copies of biohazard agents. Also, it would be valuable to have a general approach to detect the changes in fluorescence intensity upon hybridization. The increased brightness of fluorophores near metal particles provides a good opportunity to study the kinetic of DNA hybridization.
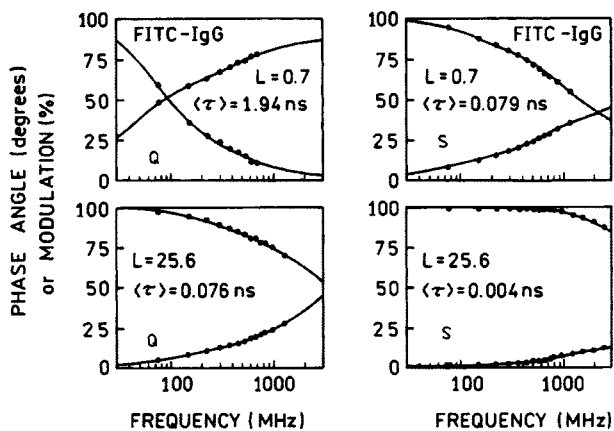

Fig. 13. Frequency-domain intensity decays of Fl-IgG on quartz (left) and silver (right).
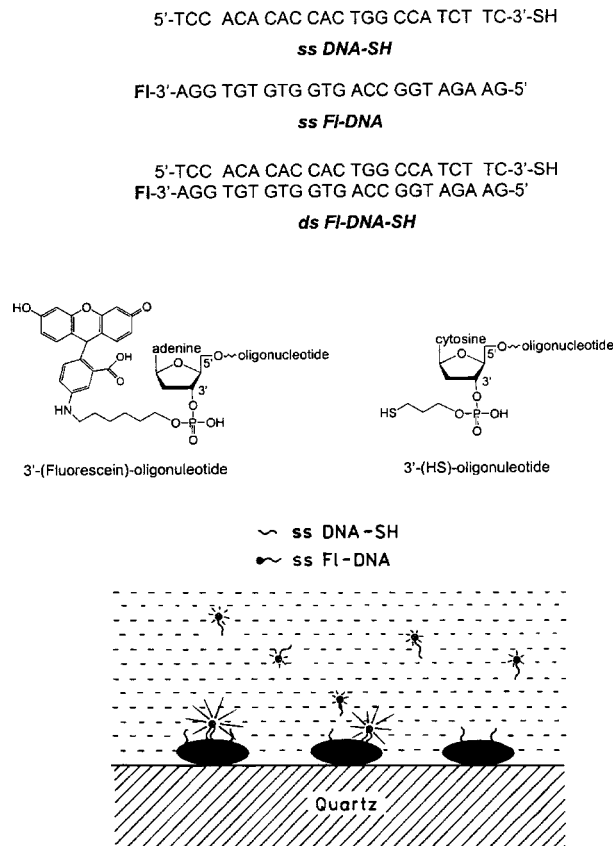

Fig. 14. Structures of DNA oligomers. The lower panel shows a schematic of the oligomers bound to silver particles.

Figure 14 (top) shows the sequence and structure of the oligomers used in these experiments. The thiolated oligonucleotide ss DNA-SH was used as the capture sequence which bound spontaneously to the silver particles. The sample containing the silver-bound DNA was positioned in a fluorometer (Fig. 15, bottom) followed by the addition of 18 nM ss Fl-DNA, which is an amount approximately equal to the amount of silver-bound capture DNA.

The fluorescence intensity began to increase immediately upon mixing and leveled off after about 20 min (Fig. 15, top). We believe this increase in intensity is due to localization of ss Fl-DNA near the silver particles by hybridization with the capture oligomer. Since metallic silver particles can increase the emission intensity of many fluorophores, this result suggests that localization of labeled oligomers near silver particles can be used in a wide range of hybridization assays. In control experiments we hybridized ss DNA-SH with ss Fl-DNA prior to deposition on silver particles. We found a similar 12-fold increase in intensity upon immobilization on silver as compared to
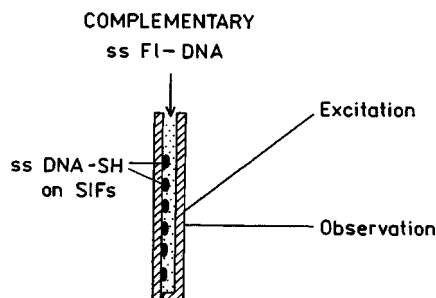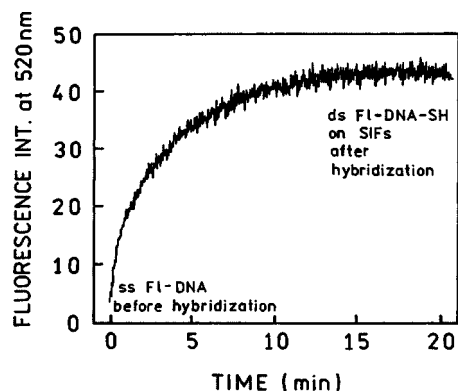
Fig. 15. Time-dependent hybridization of ss Fl-DNA to ss DNA-SH. The lower panel shows the sample configuration.
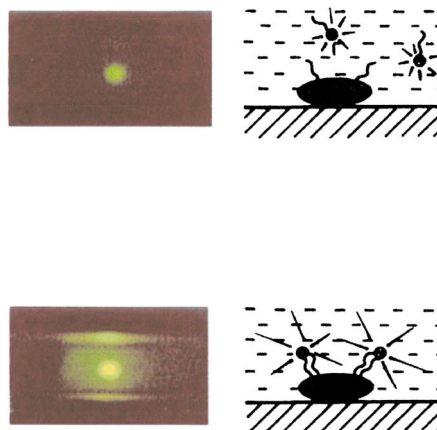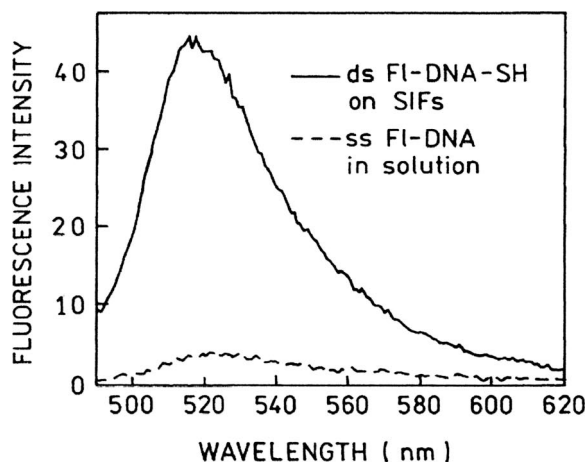

Fig. 16. Emission spectra of ss Fl-DNA in solution (dashed line) and bound (solid line) to silver particles. Roughly the same number of molecules of ss Fl-DNA and ds Fl-DNA-SH was in the illuminated area. The lower panel shows photographs of ss Fl-DNA in solution (top) and ds Fl-DNA-SH on SIFs (bottom). Figures 14–16 are adopted from [58].

an equivalent amount of ds Fl-DNA-SH in solution. We examined the emission spectra of ss Fl-DNA before and after hybridization to form ds Fl-DNA-SH (Fig. 16). The fluorescence intensity was found to be 12-fold higher for the bound form.

In our opinion, metal-enhanced fluorescence is useful for a wide range of DNA analysis formats. A metal-bound oligomer could serve as a capture probe. A labeled oligomer could bind to both the capture DNA and the target sequence. Presence of the target sequence would bring the labeled oligomer closer to the silver and enhance its fluorescence. Alternatively, hybridization of the target and labeled oligomers could be performed in solution followed by hybridization to a capture oligomer bound to the silver particles. For more details on DNA hybridization to SIFs, see [58]. The above described method can also be used to study the binding kinetic in any immunoassay.

Review of Other Systems Studied on SIFs

In several molecular systems we detected increased brightness accompanied by shorter lifetimes when deposited on SIFs. These include metal-ligand complex-doped PVA spin-coated on SIFs [59]. $[Ru(bpy)_3]^{2+}$ shows a several-fold higher quantum efficiency on SIFs than on unsilvered quartz. This indicates that metal-enhanced fluorescence occurs for long lifetime fluorophores.

In another study we show that stained DNA shows increased brightness, shorter lifetime, and better photostability on SIFs [60]. YOYO-1-labeled DNA is about an order of magnitude brighter on SIFs than on quartz. An interesting finding was that long-wavelength dye emission can be enhanced on SIFs as well [61]. Indocyanine Green (ICG), an important dye used in medical imaging, shows about a 20-fold enhancement in brightness and significantly shorter lifetimes on SIFs. The stronger enhancement observed for ICG than for other dyes can be attributed to an originally lower quantum yield. The increase in Γ_m results in a larger factor of quantum yield increase near SIFs (see Scheme 1). Overall, an increase in brightness of about one order of magnitude is possible with dyes deposited in monolayers near SIFs.
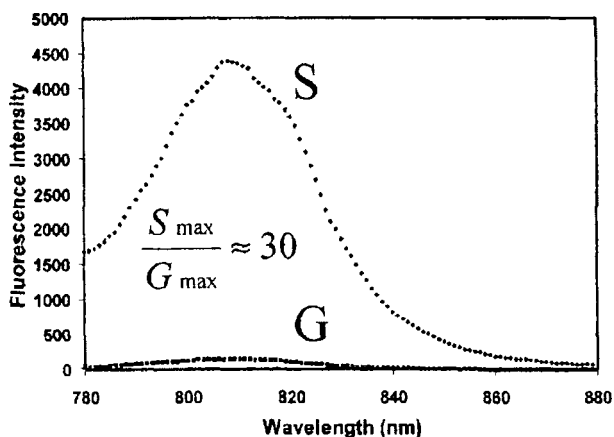
Fig. 17. Fluorescence intensity of HSA-ICG coated glass, G, and silver colloids, S, Exc = 760 nm. Adopted from [66].

Silver Colloid Coated Surfaces (SCCS)

SIFs are usually formed by reduction of silver nitrate with D-glucose [19]. Such a preparation results in a rather wide distribution of silver particles sizes. More homogeneous and slightly smaller metal particles can be achieved with deposition of metal colloids on the surface. This results in particles with a 20–30 nm diameter [62–65]. We observed that under carefully controlled experimental conditions, it is possible to achieve particle aggregates of metal colloids on the substrate surface. Our first experiment was with SCCS targeted to an ICG marker [66]. We observed about a 50% higher enhancement in brightness (Fig. 17) than with similar systems on SIFs (see Review of other systems studied on SIFs). However, we noticed that the observed enhancements are dependent on the density of deposited particles in both SIFs and SCCS preparations.

Comparison of Fluorescence Enhancements on SIFs and SCCS

In order to compare the enhancement properties of SIFs and SCCS, we prepared surfaces with comparable optical densities for both SIFs and SCCS (Fig. 18). SCCS absorption clearly indicates the presence of elongated colloid aggregates. We note that it is possible to obtain a more uniform colloid surface which differs slightly in color and has a more narrow absorption centered at 410 nm. This silver surface is not as effective as SCCS containing aggregates or SIFs. We deposited a monolayer of Texas Red-labeled bovine serum albumin (TR-BSA) on both, SIFs and SCCS surfaces. We compared the fluorescence signals for SIFs and SCCS under the same excitation/observation conditions (Fig. 19). The signal on SCCS is almost twice as strong as that on SIFs [67]. Next, we measured lifetimes and again found that the intensity decays on SCCS are more affected than on SIFs (Fig. 20). In addition, the residual long-component of intensity decay is no longer present on SCCS.

We also compared fluorescein over-labeled human serum albumin (Fl-HSA) deposited on SIFs and SCCS (Fig. 21). Again, the brightness of Fl-HSA on SCCS is at least two-fold higher than on SIFs. Higher enhancements observed for Fl-HSA than for TR-BSA are the result of the release of self-quenching in the case of the highly labeled Fl-HSA system (see Release of Self-Quenching). In conclusion, one can double the enhancements measured on SIFs by careful preparation of SCCS.

Silver-Nanorod Coated Surfaces

We have developed two preparation procedures for silver nanorod coated surfaces for surface enhanced fluorescence studies [68]. The first method enables nanorods to be readily grown in solution, which can then be deposited on APS coated glass slides, a technique which we have also used to surface immobilize solution produced silver colloids [66]. The second method enables silver nanorods to be rapidly grown in-situ, directly onto the APS coated glass slide [68], reducing deposition times from days to only a few hours. Both methods typically yield silver rods approximately 50 nm long by 20 nm
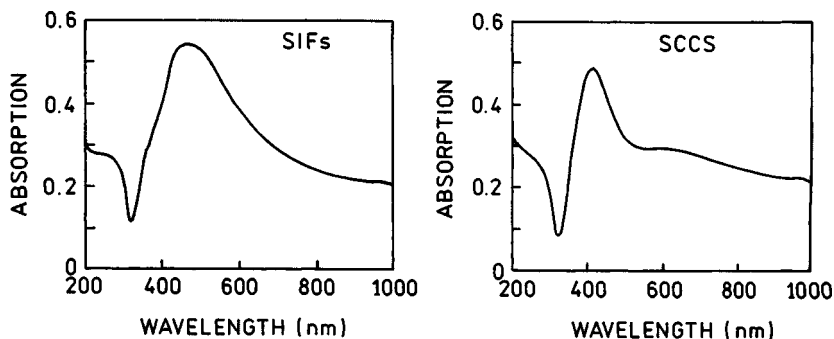

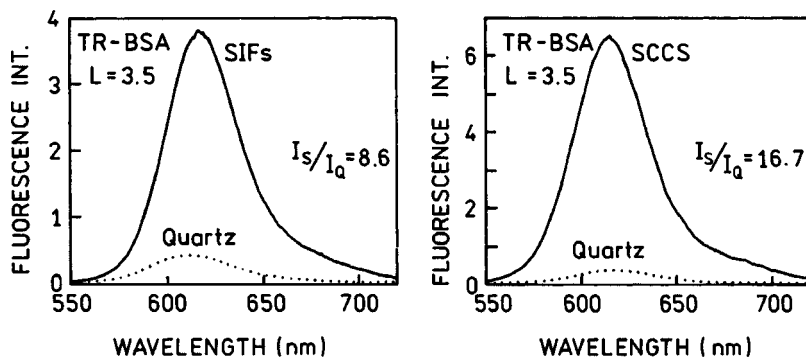**Fig. 18.** Absorption spctra of SIFs (left) and SCCS (right).

Fig. 19. Emission spectra of Texas Red-labeled BSA (TR-BSA) measured on SIFs (left) and SCCS (right).

wide (Fig. 22). The absorption spectra for silver nanorods are somewhat different than their silver colloid counterparts, similarly showing a ca. 420 nm transverse absorption band, with an additional ca. 580 nm longitudinal absorption (Fig. 22, bottom). Similarly to silver colloid surfaces, silver nanorod coated surfaces show density dependent fluorescence enhancements when coated with ICG-

protein monolayers (Fig. 23) with greater than 11-fold fluorescence enhancements with longitudinal rod surface optical densities, A_{650}, of less than 0.2.

Silver-Triangle Coated Surfaces

It is also possible to grow surface immobilized silver triangles from silver seeds, in an analogous manner to silver nanorods (Fig. 22, bottom) [69]. The absorption spectra however are somewhat different, showing two principle bands at ca, 450 and 550 nm. Similarly to silver colloid and silver rod coated glass surfaces, a silver nanostructure surface density dependence on fluorescence enhancement is observed (Fig. 24). However, in contrast to both silver colloids and rods, triangles show much greater enhancements with similar ICG-protein monolayers (Fig. 24) for similar surface optical densities.
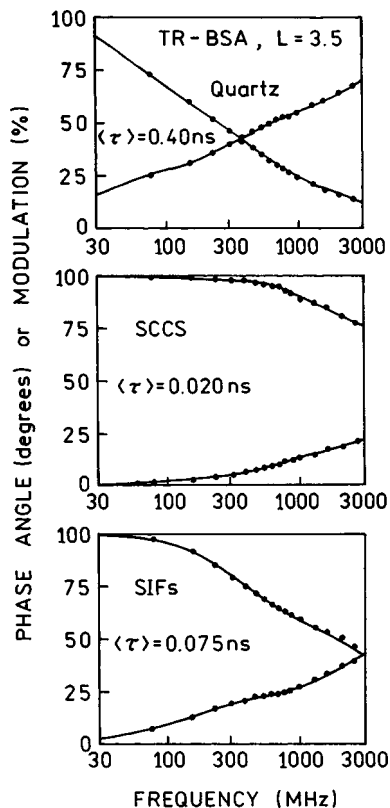

Fig. 20. Frequency-domain lifetimes of TR-BSA on quartz (top), SCCS (middle) ans SIFs (bottom).
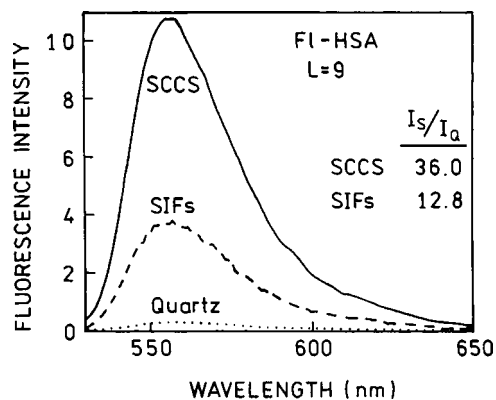

Fig. 21. Emission spectra of highly labeled Fl-HSA measured on quartz (dotted line), SIFs (dashed line) and SCCS (solid line). Figures 18–21 are adopted from [67].
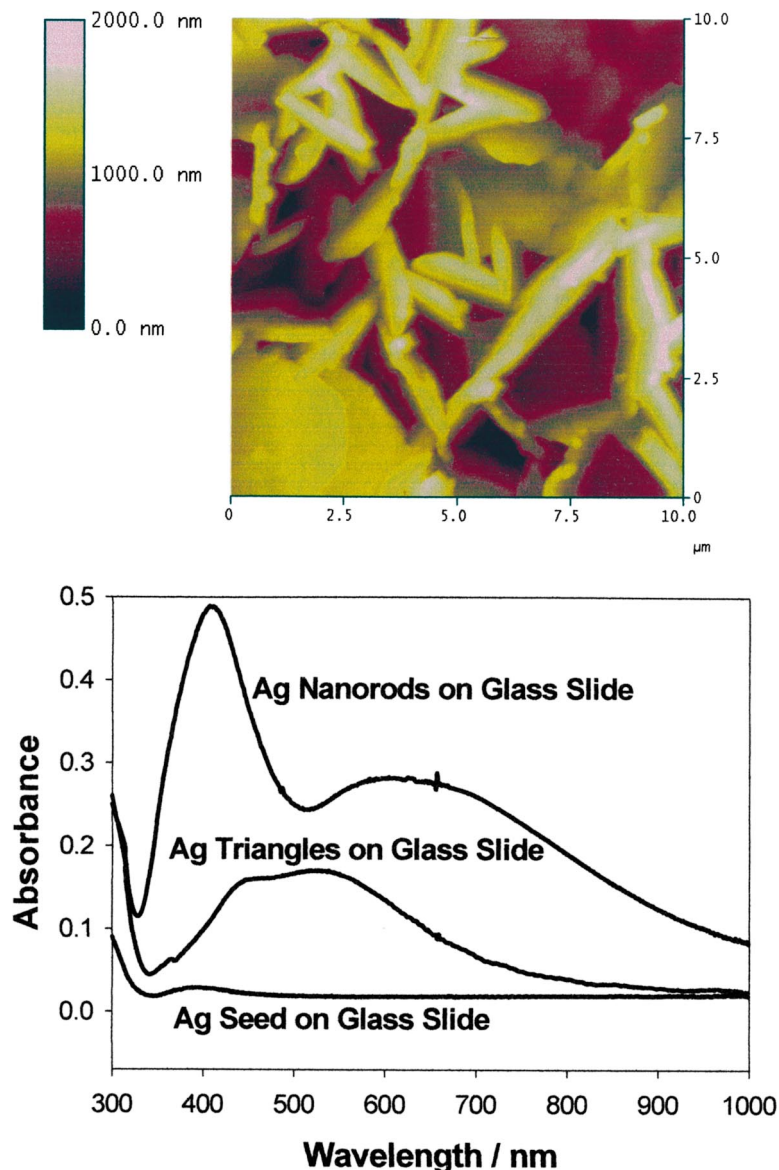
Fig. 22. AFM image of silver nanorods deposited on glass substrate (top) and absorption
spectra of silver nanorods, triangles and seeds deposited on glass substrate (bottom).

Other Methods for Silver Deposition

Photodeposition

It is known that light induces the reduction of silver salt to metallic silver. Exposure of the solution to ambient or laser light typically results in the formation of silver colloids in suspension or on the glass surface. We tested the possibility of metal-enhanced fluorescence at a desired location using a focused laser beam [70]. The experimental setup for laser deposition of silver is shown in Fig. 25. We measured a 7-fold increased intensity of ICG-HSA deposited on the silvered spot accompanied by a decreased lifetime and increased photostability. These results demonstrate the possibility of photolithographic preparation of surfaces for enhanced fluorescence in microfluidics, medical diagnostics, lab-on-a-chip and other applications.

Electrochemical Deposition

We realized that silver particles could be readily deposited on indium tin oxide (ITO), a very useful and almost
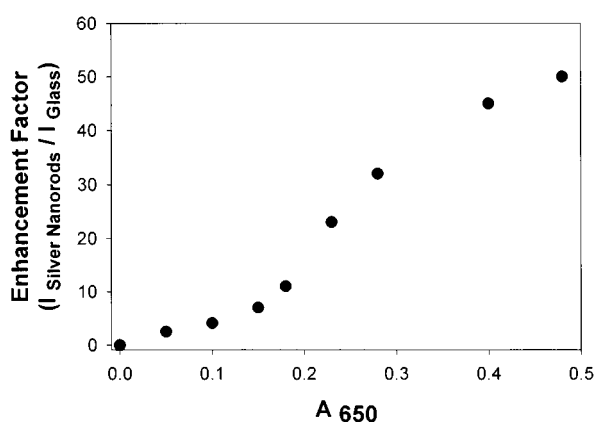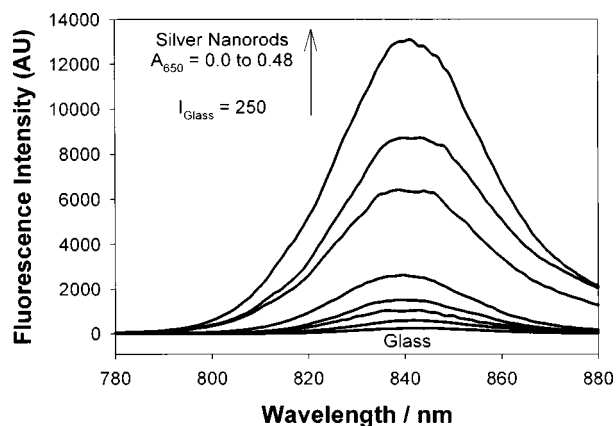
Fig. 23. Fluorescence emission intensity of HSA-ICG on silver nanorods (top) and enhnacement factor vs the absorption of silver nanorods measured at 650 nm.
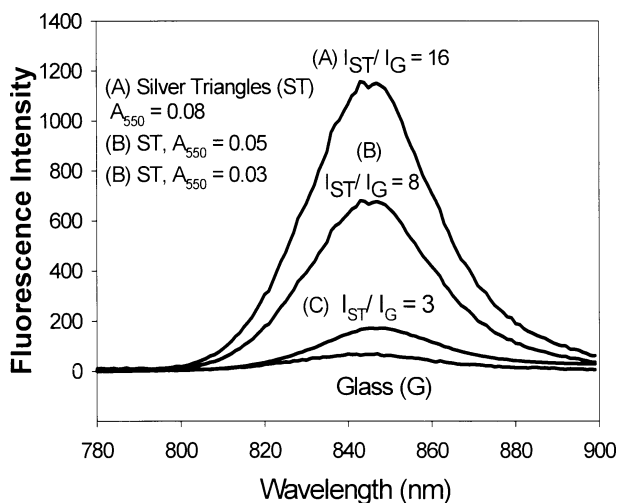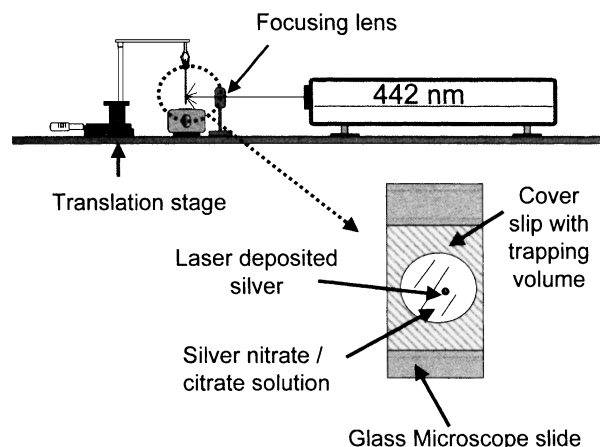

Fig. 25. Experimental setup for laser deposition of silver on APS coated glass microscope slides. Adopted from [70].

visually transparent semiconductor substrate. The absorption spectrum of electrochemically deposited silver particles is shown in Fig. 26. The insert in this figure shows a scheme for electrochemical deposition of silver on an ITO surface. The second band in the absorption spectrum near 550nm indicates the presence of larger silver particles than usually obtained for SIFs or SCCS. In fact, the AFM image (Fig. 27) confirms this observation. The 5-fold enhancement observed on the prepared substrates [71] was somehow smaller than for other silver surfaces. We believe, however, that once improved electrochemical deposition can be a very reliable, easily controllable and useful method.

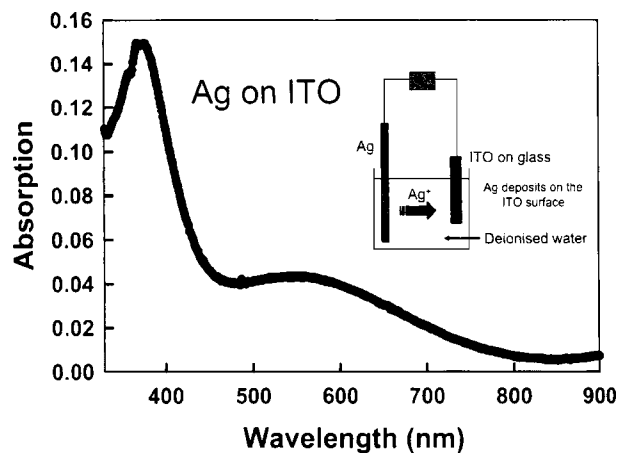**Fig. 24.** Fluorescence emission intensity of HSA-ICG on silver triangles.

Fig. 26. Absorption spectrum of silver-coated ITO produced via electrochemical deposition. ITO without silver was in the reference beam. The insert shows the scheme for electrochemical deposition of Ag on an ITO surface.
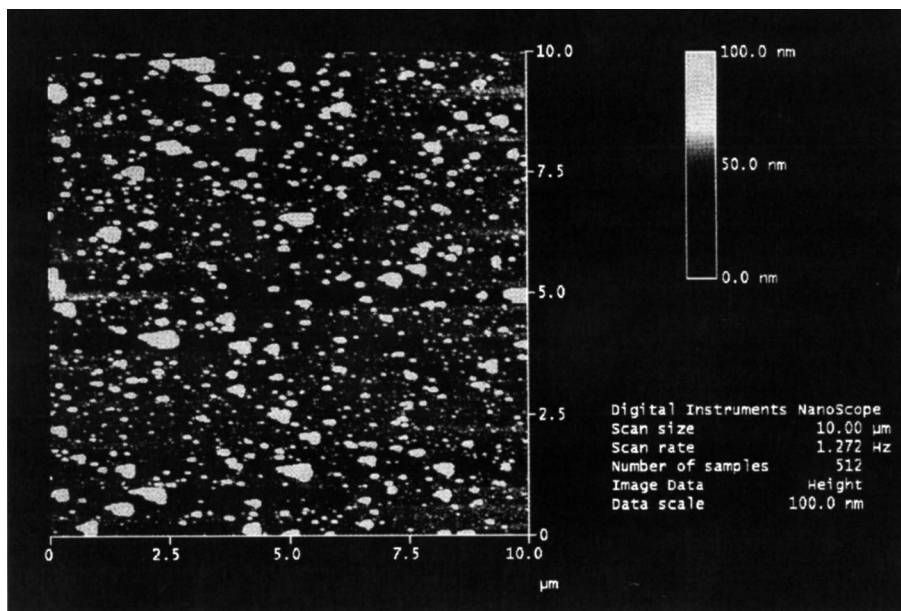
Fig. 27. AFM image of the silver coated ITO surface produced by electrolysis. Figures 26–27 are adopted
from [71].

Silver Fractal-Like Nanostructures

Some of our largest enhancements to date have been
observed from fluorophore-protein coated silver fractal-
like structures [72–74]. By passing an electric current be-

Fig. 28. Constant current apparatus for electrode silver fractal growth
(top). Silver growth on glass slide (bottom).

tween two silver electrodes in deionised water, silver frac-
tal like structures rapidly grow from the cathode (Fig. 28).
We have subsequently been able to study roughened sil-
ver electrodes (cathode) [72,73] or surfaces which have the
fractals adhered too in-situ [74]. Both surfaces show spa-
tially localized enhancements (hot-spots) of many 1000-
fold when coated (Figs. 29, 30). Even the spatially aver-
aged surface intensities reveal fluorescence enhancement
values in the 100's, with dramatically reduced lifetimes
and an increased probe photostability. The silver fractals
can be simply grown on-demand, making this an ideal
technology for surface assays, field deployable biosensors
as well as lab-on-a-chip type technologies.

CONCLUSIONS

The fluorescence emission of fluorophores is strongly
affected by near by metal particles. The metal particle-
fluorophore interaction is through-space, with maximum
brightness enhancement at distance of about 70–100 Å.
The magnitude of enhancement depends on a quantum
yield of fluorophore and metalized surface. The density
and shape of metal particles play an important role in
the brightness enhancement. The increase in brightness
is accompanied by a shortening of lifetimes and often by
higher photostability. The enhancement in brightness can
be used in various assays such as DNA hybridization or
immunoassays and to control the flow in microfluidics.

Fig. 29. Silver nanostructures deposited on glass during electroplating (A). Panels B and C are consecutive magnification of the marked area on panel A. Bright field image.

The strongest benefits will be for chromophores with extremely low quantum efficiencies like DNA bases. One may also expect the applications of metal enhanced fluorescence in imaging and single molecule counting.
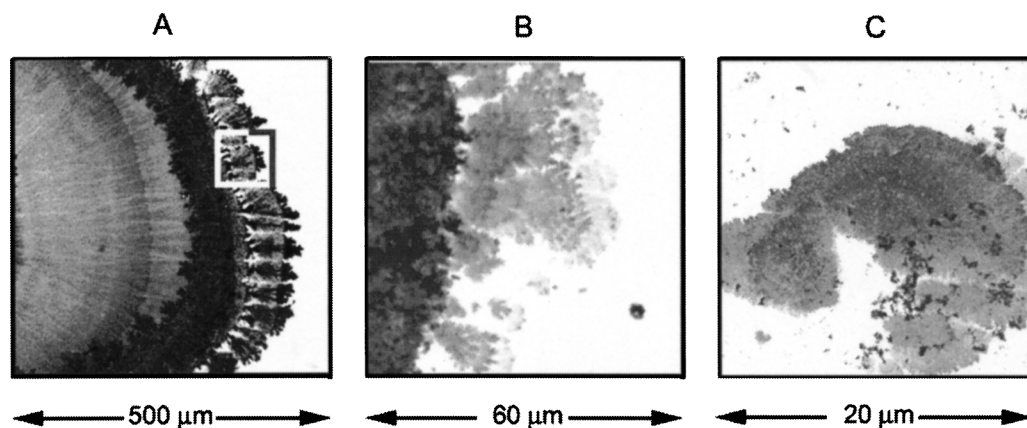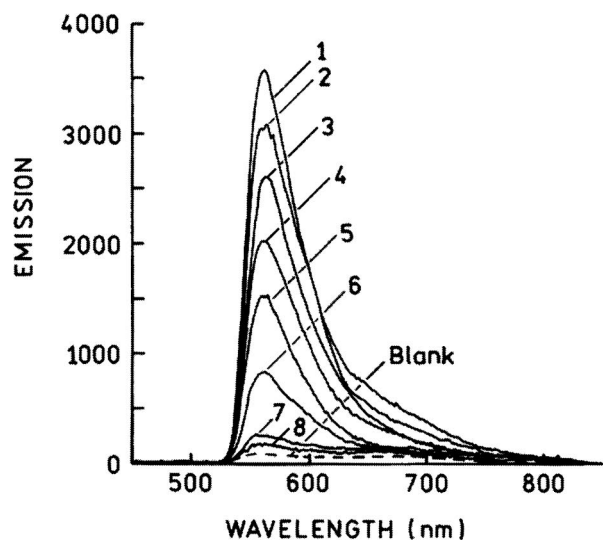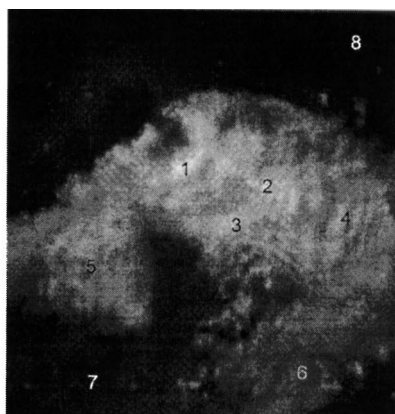
ACKNOWLEDGMENTS

Fig. 30. Fluorescence image of Fl-HSA deposited on the silver structure shown in Fig. 29C (top). Emission spectra of the numbered areas shown above (bottom). Figures 29–30 are adopted from [74].

REFERENCES

1. K. H. Drexhage (1974). in E. Wolfe (Ed.), *Progress in Optics*, North-Holland, Amsterdam, pp. 161–323.
2. D. A. Weitz, S. Garoff, C. D. Hansen, and T. J. Gramila (1982). Fluorescent lifetimes of molecules on silver-island films. *Opt. Lett.* **7**(2), 89–91.
3. F. R. Aussenegg, A. Leitner, M. E Lippitsch, H. Reinish, and M. Reigler (1987). Novel aspects of fluorescence lifetime for molecules positioned close to metal surfaces. *Surf. Sci.* **139**, 935–945.
4. A. Leitner, M.E. Lippitsch, S. Draxler, M. Reigler, and F.R. Aussenegg (1985). Fluorescence properties of dyes absorbed to silver islands, investigated by picosecond techniques, *Appl. Phys. B* **36**, 106–109.
5. J. Gersten and A. Nitzan (1981). Spectroscopic properties of molecules interacting with small dielectric particles. *J. Chem. Phys.* **75** (3), 1139–1152.
6. D. A. Weitz, S. Garoff, J. I. Gersten, and A. Nitzan (1983). The enhancement of Raman scattering, resonance Raman scattering, and fluorescence from molecules absorbed on a rough silver surface. *J. Chem Phys.* **78**(9), 5324–5338.
7. M. Fleischmann, P. J. Hendra, and A. J. McQuillan (1974). Raman spectra of pyridine absorbed at a silver electrode, *Chem Phys. Letts.* **26**(2), 163–166.
8. D. L. Jeanmaire and R. P. Van Duyne (1977). Surface Raman spectroelectrochemistry. Part 1. Heterocyclic, aromatic, and aliphtaic

amines adsorbed on the anodized silver electrode, *J. Elecroanal. Chem.* **84**, 1–20.

9. B. Pettingar and A. Gerolymatou (1984). Dyes adsorbed at Ag-colloids: Substitution of fluorescence and surface Raman scattering. *Ber. Bunges. Phys. Chem.* **88**, 359–363.

10. K. Kneipp, H. Kneipp, I. Itzkan, R. R. Dasari, and M. S. Feld (1999). Surface-enhanced Raman scattering: A new tool for biochemistry spectroscopy. *Curr. Sci.* **77**(7), 915–924.

11. T. Vo-Dinh, D. L. Stokes, G. D. Griffin, M. Volkan, U. J. Kim, and M. I. Simon (1999). Surface-enhanced Raman scattering (SERS) method and instrumentation for genomics and biomedical analysis. *J. Raman Spectrosc.* **30**, 785–793.

12. T. Vo-Dinh (1998). Surface-enhanced Raman spectroscopy using metallic nanostructures. *Trends Anal. Chem.* **17**(8–9), 557–582.

13. S. Nie and S. R. Emory (1997). Probing single molecules and single nanoparticles by surface-enhanced Raman scattering. *Science* **275**, 1102–1106.

14. K. Kneipp, H. Kneipp, V. Bhaskaran Kartha, R. Manoharan, G. Deinum, I. Itzkan, R. R. Dasari, and M. S. Feld (1998). Detection and identification of a single DNA base molecule using surface-enhanced Raman scattering (SERS). *Phys. Rev. E* **57**(6), R6281–R6284.

15. J. R. Lakowicz (2001). Radiative decay engineering: Biophysical and biomedical applications. *Anal. Biochem.* **298**, 1–24.

16. J. R. Lakowicz, I. Gryczynski, Y. Shen, J. Malicka, and Z. Gryczynski (2001). Intensified fluorescence. *Photonics Spectra*, October 2001, 96–104.

17. J. R. Lakowicz, J. Malicka, I. Gryczynski, Z. Gryczynski, and C. Geddes (2003). Radiative decay engineering: The role of photonic mode density in biotechnology, *J. Phys. D Appl. Phys.* **36**, R240–R249.

18. I. Gryczynski, J. Malicka, Y. Shen, Z. Gryczynski, and J. R. Lakowicz (2002). Multiphoton excitation of fluorescence near metallic particles: enhanced and localized excitation. *J. Phys. Chem.* **106**, 2191–2195.

19. J. R. Lakowicz, Y. Shen, S. D'Auria, J. Malicka, J. Fang, Z. Gryczynski, and I. Gryczynski (2002). Radiative decay engineering: Effects of silver island films on fluorescence intensity, lifetimes, and resonance energy transfer. *Anal. Biochem.* **301**, 261–277.

20. J. Malicka, I. Gryczynski, B.P. Maliwal, J. Fang, and J. R. Lakowicz (2003). Fluorescence spectral properties of cyanine dye labeled DNA near metallic silver particles. *Biopolym. (Biospectrosc.)* **72**, 96–104.

21. J. R. Lakowicz, B. P. Maliwal, J. Malicka, Z. Gryczynski, and I. Gryczynski (2002). Effects of Silver Island Films on the luminescent intensity and decay times of lanthanide chelates. *J. Fluorescence.* **12**, 431–437.

22. B. P. Maliwal, J. Malicka, I. Gryczynski, Z. Gryczynski, and J. R. Lakowicz (2003). Fluorescence properties of labeled proteins near silver colloid surfaces, *Biopolym. (Biospectrosc.)* **70**, 585–594.

23. J. Malicka, I. Gryczynski, J. Fang, and J.R. Lakowicz (2003). Fluorescence spectral properties of cyanine dye-labeled DNA oligomers on surfaces coated with silver particles. *Anal. Biochem.* **317**, 136–146.

24. J. R., Lakowicz, J. Malicka, and I. Gryczynski (2003). Silver particles enhance emission of fluorescent DNA oligomers. *BioTechniques* **34**, 62–68.

25. S. A. Soper, H. L. Nutter, R. A. Keller, L. M. Davis, and E. B. Shera (1993). The photophysical constants of several fluorescent dyes pertaining to ultrasensitive fluorescence spectroscopy. *Photochem. Photobiol.* **57**, 972–977.

26. C. Eggeling, J. Widengren, R. Rigler, and C. A. M. Seide (1999). In W. Retting, B. Strehmel, S. Schrader, and H. Seifert (Eds.), *Applied Fluorescence in Chemistry, Biology and Medicine. MAFS Proceedings Book*, Springer-Verlag, New York, 562 pp.

27. A. Wokaun, H.-P. Lutz, A. P. King, U. P. Wild, and R. R. Ernst (1983). Energy transfer in surface enhanced fluorescence. *J. Chem. Phys.* **79**, 509–514.

28. P. J. Tarcha, J. DeSaja-Gonzalez, S. Rodriquez-Llorente, and R. Aroca (1999). Surface- enhanced fluorescence on SiO$_2$ coated silver island films, *Appl. Spectrosc.* **53**, 43–48.

29. A. E. German and G.A. Gachko (2001). Dependence of the amplification of giant Raman scattering and fluorescence on the distance between an adsorbed molecule and a metal surface. *J. Appl. Spectrosc.* **68**, 987–992.

30. K. Sokolov, G. Chumanov, and T. M. Cotton (1998). Enhancement of molecular fluorescence near the surface of colloidal metal films. *Anal. Chem.* **70**, 3898–3905.

31. J. Malicka, I. Gryczynski, Z. Gryczynski, and J. R. Lakowicz (2003). Effects of fluorophore-to-silver distance on the emission of cyanine-dye-labeled oligonucleotides. *Anal. Biochem.* **317**, 57–66.

32. R. C. Ebersole, J. A. Miller, J. R. Moran, and M. D. Ward (1990). Spontaneously formed functionally active avidin monolayers on metal surfaces: A strategy for immobilizing biological reagents and design of piezoelectric biosensors. *J. Am. Chem. Soc.* **112**, 3239–3241.

33. J. Jablonski (1955). Self-depolarization and decay of photoluminescence of solutions. *Acta Phys. Pol.* **XIV**, 295–307.

34. C. Bojarski, J. Grabowska, L. Kulak, and J. Kusba (1991). Investigations of the excitation energy transport mechanism in donor-acceptor systems. *J. Fluoresc.* **1**, 183–191.

35. R. S. Knox (1968). Theory of polarization quenching by excitation transfer. *Physica* **39**, 361–386.

36. P. Bojarski, L. Kulak, C. Bojarski, and A. Kawski (1995). Non-radiative excitation energy transport in one-component disordered systems. *J. Fluoresc.* **5**, 307–319.

37. R. E. Dale and R. K. Bauer (1971). Concentration depolarization of the fluorescence of dyestuffs in viscous solution. *Acta Phys. Pol. A* **40**, 853–882.

38. C. R. Gocanour and M. D. Fayer (1981). Electronic excited state transport in random systems. Time-resolved fluorescence depolarization measurements. *J. Phys. Chem.* **85**, 1989–1994.

39. A. Kawski (1983). Excitation energy transfer and its manifestation in isotropic media, *Photochem. Photobiol.* **38**, 487–508.

40. I. A. Hemmila (1991). *Applications of Fluorescence in Immunoassays*, *Wiley*, New York, p. 113.

41. X. Zhuang, T. Ha, H. D. Kim, T. Centner, S. Labeit, and S. Chu (2000). Fluorescence quenching: A tool for single-molecule protein-folding study, *PNAS* **97**, 14241–14244.

42. S. Kalinin, J. G. Molotkovsky, and L. B.-A. Johansson (2003). Distance measurements using partial donor-donor energy migration with pairs of fluorescent groups in lipid bilayers. *J. Phys. Chem. B* **107**, 3318–3324.

43. L. W. Runnels and S. F. Scarlata (1995). Theory and application of fluorescence homotransfer to melittin oligomerization. *Biophys. J.* **69**, 1569–1583.

44. J. Karolin, M. Fa, M. Wilczynska, T. Ny, and L.B.-A. Johansson (1998). Donor-donor energy migration for determining intramolecular distances in proteins I. Application of a model to the latent plasminogen activator inhibitor-1 (PAI-1). *Biophys. J.* **74**, 11–21.

45. G. C. Visor and S. D. Schulman (1981). Fluorescence immunoassay. *J. Pharm. Sci.*, **70**, 469–475.

46. T. Vo-Dinh, M. J. Sepaniak, G. D. Griffin, and J. P. Alarie (1993). Immunosensors: Principles and applications. *Immunomethods*, **3**, 85–92.

47. M. N. Kronick and P. D. Grossman (1983). Immunoassay techniques with fluorescent phycobiliprotein conjugates. *Clin. Chem.* **29**, 1582–1586.

48. E. Soini and H. Kojola (1983). Time-resolved fluorometer for lanthanide chelates–a new generation of nonisotropic immunoassays. *Clin. Chem.* **29**, 65–68.

49. J. R. Lakowicz, J. Malicka, S. D'Auria, and I. Gryczynski (2003). Release of the self-quenching of fluorescence near silver metallic surfaces. *Anal. Biochem.* **320**, 13–20.

50. J. Malicka, I. Gryczynski, and J. R. Lakowicz (2003). Enhanced emission of highly labeled DNA oligomers near silver metallic surfaces. *Anal. Chem.* **75**, 4408–4414.

51. J. R. Lakowicz, J. Malicka, J. Huang, Z. Gryczynski, and I. Gryczynski (in press). Ultra-bright fluorescein labeled antibodies near silver metallic surfaces. *Biopolym.*

52. L. E. Morrison (2003). In J. R. Lakowicz (Ed.), *Topics in Fluorescence Spectroscopy*, *Vol. 7*, Kluwer Academic/Plenum Press, New York, pp. 69–103.

53. P. O. Brown and D. Botstein (1999). Exploring the new world of the genome with DNA microarrays. *Nat. Genet. Suppl.* **21**, 33–37.

54. M. Schena, R. A. Heller, T. P. Theriault, K. Konrad, E. Lachenmeier, and R. W. Davis (1998). Microarrays: Biotechnology's discovery platform for functional genomics. *TIBTECH* **16**, 301–306.

55. F. Komurian-Pradel, G. Paranhos-Bacala, M. Sodoyer, P. Chevallier, B. Mandrand, V. Lotteau, and P. Andre (2001). Quantitation of HCV RNA using real-time PCR and fluorimetry. *J. Virol. Methods* **95**, 111–119.

56. N. J. Walker (2002). A technique whose time has come. *Science* **296**, 557–559.

57. M. J. Difilippantonio and T. Ried (2003). In J. R. Lakowicz (Ed.), *Topics in Fluorescence Spectroscopy*, *Vol. 7*, Kluwer Academic/Plenum Press, New York, pp. 291–316.

58. J. Malicka, I. Gryczynski, and J. R. Lakowicz (2003). DNA hybridization assays using metal-enhanced fluorescence. *Biochem. Biophys. Res. Commun.* **306**, 213–218.

59. I. Gryczynski, J. Malicka, E. Holder, N. DiCesare, and J. R. Lakowicz (2003). Effects of metallic silver particles on the emission properties of $[Ru(bpy)_3]^{2+}$. *Chem. Phys. Lett.* **372**, 409–414.

60. J. R. Lakowicz, J. Malicka, and I. Gryczynski (2003). Increased intensities of YOYO-1-labeled DNA oligomers near silver particles. *Photochem. Photobiol.* **77**, 604–607.

61. J. Malicka, I. Gryczynski, C. Geddes, and J.R. Lakowicz (2003). Metal-enhanced emission from indocyanine green: a new approach to *in vivo* imaging. *J. Biomed. Opt.* **8**, 472–478.

62. K. Sokolov, G. Chumanov, and T. M. Cotton (1998). Enhancement of molecular fluorescence near the surface of colloidal metal films. *Anal. Chem.* **70**, 3898–3905.

63. J. Turkevich, P. C. Stevenson, and J. Hillier (1951). A study of the nucleation and growth processes in the synthesis of colloidal gold. *J. Discuss. Faraday Soc.* **11**, 55–75.

64. A. Henglein and M. Giersig (1999). Formation of colloidal silver particles: Capping action of citrate. *J. Phys. Chem. B* **103**, 9533–9539.

65. L. Rivas, S. Sanchez-Cortes, J. V. Garcia-Romez, and G. Morcillo (2001). Growth of silver colloidal particles obtained by citrate reduction to increase the Raman enhancement factor. *Langmuir* **17**, 574–577.

66. C. Geddes, H. Cao, I. Gryczynski, Z. Gryczynski, J. Fang, and J. R. Lakowicz (2003). Metal-enhanced fluorescence (MEF) due to silver colloids on a planar surface: Potential applications of Indocyanine Green to in vivo imaging. *J. Phys. Chem. A* **107**, 3443–3449.

67. J. Lukomska, J. Malicka, I. Gryczynski, and J. R. Lakowicz (2004). Fluorescence enhancements on silver colloid coated surfaces. *J. Fluoresc.* **14**, 417–424.

68. K. Aslan, J. R. Lakowicz, and C. D. Geddes (in preparation). Rapid growth of silver nano-rods on surfaces for applications in metal-enhanced fluorescence. *J. Phys. Chem. B.*

69. K. Aslan, J. R. Lakowicz, and C. D. Geddes (in preparation). Rapid growth of silver triangles for surface-enhanced fluorescence. *Appl. Spectrosc.*

70. C. Geddes, A. Parfenov, and J. R. Lakowicz (2003). Photodeposition of silver can result in metal-enhanced fluorescence. *Appl. Spectrosc.* **57**, 526–531.

71. C. Geddes, A. Parfenov, D. Roll, J. Fang, and J. R. Lakowicz (2003). Electrochemical and laser deposition of silver for use in metal-enhanced fluorescence. *Langmuir* **19**, 6236–6241.

72. C. D. Geddes, A. Parfenov, D. Roll, I. Gryczynski, J. Malicka, and J. R. Lakowicz (2003). Silver fractal-like structures for metal-enhanced fluorescence: Enhanced fluorescence intensities and increased probe photostabilities. *J. Fluoresc.* **13**, 267–276.

73. C. D. Geddes, A. Parfenov, D. Roll, I. Gryczynski, J. Malicka, and J. R. Lakowicz (in press). Roughened silver electrodes for use in metal-enhanced fluorescence. *Spectrochem. Acta A.*

74. A. Parfenov, I. Gryczynski, J. Malicka, C. D. Geddes, and J. R. Lakowicz (2003). Enhanced fluorescence from fluorophores on fractal silver surfaces. *J. Phys. Chem. B* **107**, 8829–8833.